ISSN 1068-3755, Surface Engineering and Applied Electrochemistry, 2016, Vol. 52, No. 4, pp. 362–369. © Allerton Press, Inc., 2016.

Influence of Iron Doping on Morphological, Structural and Optical Properties of Zinc Oxide Thin Films Prepared by Dip-Coating Method[1]

C. Zegadi[a], *, A. Abderrahmane[b], D. Chaumont[c], Y. Lacroute[c], K. Abdelkebir[d], S. Hamzaoui[a], and M. Adnane[a]

[a] *Laboratory of Electron Microscopy and Materials Sciences, University of Science and Technology of Oran, El-Mnaouer Oran, Algeria*

[b] *Organization for Research Promotion, Research Promotion Center, The University of Electro-Communications (UEC) 1-5-1 Chofugaoka Chofu, Tokyo Japan*

[c] *NanoForm–ICB, Université de Bourgogne, Dijon, France*

[d] *Equipe Surfaces, Interfaces, Procédés (SIP), Centre des Matériaux P.M. FOURT, École des Mines de Paris–MINES Paris Tech, Paris, France*

**e-mail: chewkizegadi@gmail.com*

Received April 28, 2015; in final form, May 27, 2015

Abstract– Undoped zinc oxide and iron-doped zinc oxide thin films have been deposited by the sol-geldip-coating method. The Fe/Zn nominal volume ratio was 5% in the solution. The effects of Fe incorporation on morphological, structural, and optical properties of ZnO films were investigated. The scanning electron microscopy measurements showed that the surface morphology of the prepared thin films was affected by Fe doping. The X-ray diffraction patterns of the thin films showed that doped incorporation leads to substantial changes in the structural characteristics of ZnO thin films. The optical absorption measurements indicated a band gap in the range of 3.31 to 3.19 eV. The X-ray photoelectron spectroscopy demonstrated that Fe is incorporated in the ZnO matrix with 6.5 atomic percent (at %). The energy dispersive spectroscopy studies indicated the formation of ZnO with high efficiency.

Keywords: sol-gel dip-coating, polycrystalline ZnO, Fe-doping ZnO, scanning electron microscopy, X-ray diffraction, ultraviolet–visible spectroscopy, X-ray photoelectron spectroscopy, energy dispersive spectroscopy

DOI: 10.3103/S1068375516040128

INTRODUCTION

Zinc Oxide (ZnO) thin films have been extensively studied due to their attractive electronic and optoelectronic properties [1–3]. Doping of the ZnO thin films by suitable elements can lead to significant improvements of their optical, magnetic, and electrical properties without any change in the crystalline structure [4, 5]. Furthermore, ZnO thin films attracted a lot of attention for a variety of potential applications in both microelectronic and optoelectronic devices such as solar cells, transparent conducting oxides (TCO), ultraviolet (UV) and blue light emitters and transistors. Recently, Fe-doped ZnO has been in the focus of attention of researchers and engineers because it can expand the applications of ZnO in different domains [6–8].

In the last few years, the sol-gel deposition technique gains high intension by scientists due to its advantages such as low temperature processing. The sol-gel technique is an adequate procedure for homogeneous thin films of high purity [9, 10]; it is also efficient for the preparation of nanostructure metal oxides and it is a simple and quite low-cost processing alternative to the vacuum deposition techniques. This deposition technique is based on the hydrolysis and the polycondensation of metal organic precursors, such as metal alkoxides [9].

In this paper, we deal with the sol-gel technique for the deposition of the undoped (u-ZnO) and Fe-doped zinc oxide (ZnO:Fe) thin films. Their morphological, structural, and optical properties were investigated by the scanning electron microscopy (SEM) micrographs, X-ray diffraction (XRD) data, ultraviolet–visible (UV-VIS) spectroscopy, X-ray photoelectron

[1] The article is published in the original.

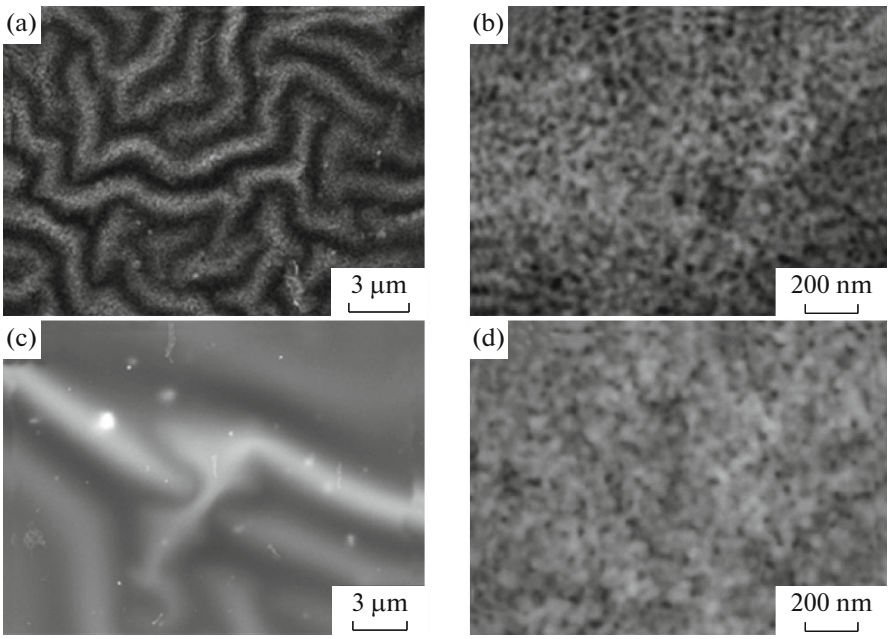

Fig. 1. SEM images of (a) and (b) ZnO:Fe thin films with magnification of 5000 and 75000, respectively, and (c) and (d) of u-ZnO thin films with magnification of 5.000 and 75.000, respectively.

spectroscopy (XPS) and energy-dispersive spectroscopy (EDS).

EXPERIMENTAL

Dip-Coating Process

The deposition of u-ZnO thin films was performed using the sol–gel dip-coating method. A starting solution with the concentration of 0.1 mL^{-1} of zinc acetated dehydrated ($Zn(CH_3COO)_2 \cdot 2H_2O$, 29088.29) dissolved in absolute ethanol (C_2H_5OH, 24103) was stirred at a speed of 250 rot./min, T 90°C for 3 hours in order to yield a transparent, homogeneous, and stable sol. We used a glass micro-slides substrate (75 × 25 × 1 mm, Super Premium Microscope Slides); the substrates were cleaned in an ultrasonic bath for 10 min. and then rinsed by ethanol [9]. The sol-gel dip-coating deposition was performed onto the prepared glass substrates at room temperature, according to the following process: the glass substrate was coated in the sol for 60 s, the speed of immersion was 5 cm min^{-1}. After each deposition, the covered substrate was heated to 100°C for 3 min. The coating procedure was repeated ten times before post heated at 580°C for 1 hour.

The deposition of ZnO:Fe thin films was performed using the same process: to the same starting solution iron (III) chloride hexahydrate ($FeCl_3 \cdot 6H_2O$, 44944) was added after 20 minutes, the time needed to get a clear and homogenous solution. The atomic concentration of Fe was 5% of Zn in the solution.

Characterization

The surfaces morphologies of the prepared u-ZnO and ZnO:Fe were examined by a VEGA3 SEM. The structural characterization of the films was analyzed using a Siemens X-ray automatic diffractometer D500 series. The diffractometer reflections were taken at room temperature and the values were swapped between 20° and 90° with the $CuK_\alpha L$ radiation and low scanning speed of 0.03°/min, with an incident wavelength of 1.54056 Å. The optical transmittance measurements of the investigated thin films were performed with UV-Visible Spectrophotometer (Thermo-electron corporation model), the optical band gaps and Urbach energies were deduced. For the optical transmittance with an integrating sphere in the wavelength range from 190 to 900 nm, the valence states of the elements in ZnO and ZnO:Fe were determined by VG Multilab 2000 XPS, and finally we used MET JEOL JEM 2100F model for the EDS characterizations.

RESULTS AND DISCUSSION

Scanning Electron Microscopy

Figure 1 shows the SEM images of ZnO:Fe (Figs. 1a, 1b) and u-ZnO (Figs. 1c, 1d). The surface of the thin films is homogeneous in all scanned areas of the samples. A ZnO:Fe film has shown an increase in the crystallite size. SEM images clearly showed that Fe-doping has an important role in changing the structure and improving the crystallinity of ZnO films [9, 11].

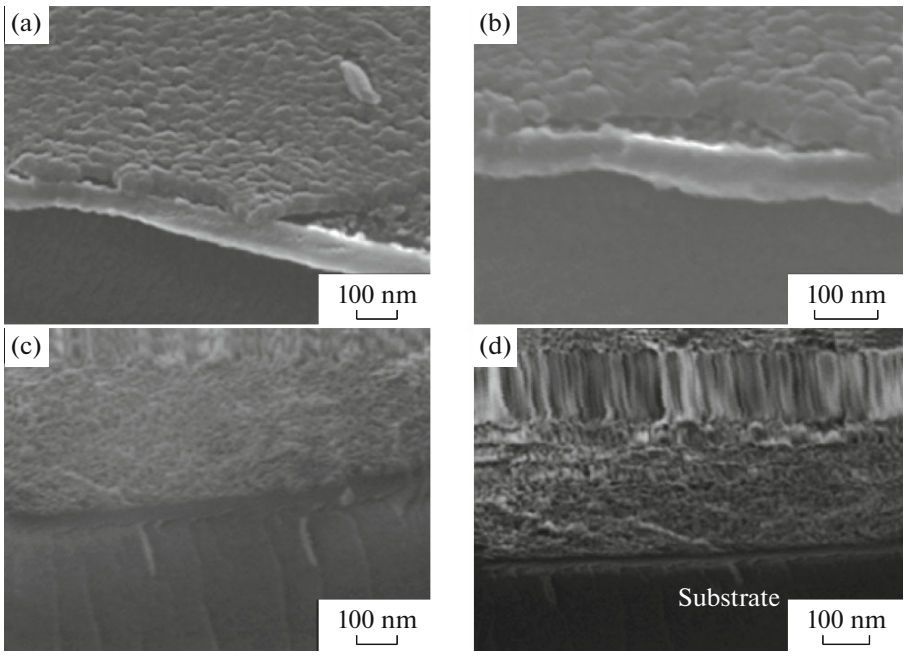

Fig. 2. SEM images of (a) and (b) ZnO:Fe thin films with magnification of 110.000 and 180.000, respectively; and (c) and (d) u-ZnO thin films with magnification of 100.000 and 120.000, respectively.

Wrinkles appeared in all samples with the same thickness but were more distinct in doped ZnO. To understand the origin of the wrinkles, both u-ZnO and ZnO Fe- thin films were cut in transverse and inclined at 45 degrees as shown in Fig. 2. The volumes and the surfaces of these layers were uniform, dense, and well sintered. Moreover, an interconnected structure of a thickness over 0.33 micrometers and a little peeling of the layer was observed in the u-ZnO, caused by a compressive stress near the surface. Furthermore, the layers of ZnO:Fe were under a compression micro-stress while the layers of u-ZnO had neither micro-wrinkles nor stress. These observations were in good agreement with the calculated stress by the XRD.

Additionally, cracks were observed in the end of the layers surfaces due to an internal stress resulting from the rapid cooling of the sample, i.e. a thermal-shock. Crusts were observed in the surface of ZnO:Fe as a result of the amorphous nature of the substrates.

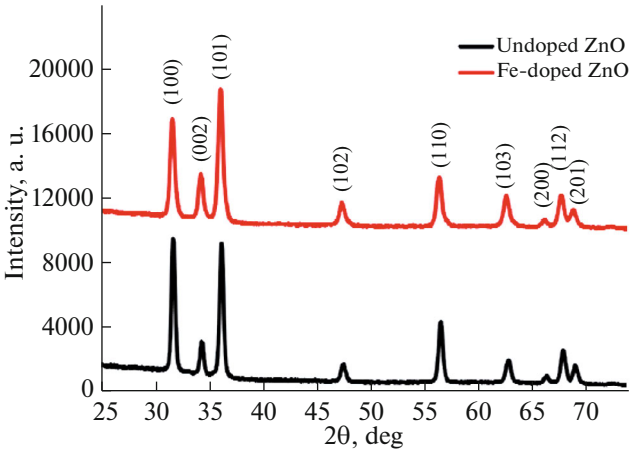

Fig. 3. XRD patterns of u-ZnO and ZnO:Fe films.

X-ray Diffraction Spectroscopy

The crystallinity and the preferred crystal orientation of both the u-ZnO and ZnO:Fe thin films were analyzed by the XRD. Figure 3 shows the XRD patterns of u-ZnO and ZnO:Fe thin films. In all samples, the peak position agrees well with the reflections of a hexagonal quartzite type structure of polycrystalline ZnO (JCPDS Card no. 36-1451). We noticed the absence of the iron oxide phase such as iron (III) oxide (Fe_2O_3) or others phases in the ZnO:Fe.

Where d_{hkl} is the lattice spacing, θ_{hkl} is the angle of the incidence or the Bragg diffraction, λ is the wavelength of the radiation, and n is the diffraction order ($n = 1, 2, ...$). The lattice constants were deduced from the XRD results using the following equation:

$$2d_{hkl} \sin \theta_{hkl} = n\lambda. \quad (1)$$

The lattice constants a and c of the u-ZnO and of the ZnO:Fe thin films are reflected in Tables 1 and 2, respectively. The lattice constants are in agreement with the standard value from the CPDS Card no. 36-1451,

Table 1. The diffraction angle (2θ), lattice spacing (*d*), intensity (*I*) and crystallite size (*D*) of u-ZnO thin films

	(*hkl*)	2θ(°)	*d*(Å)	*D*(Å)	β(°)	*I*(a.u.)	2θ(°)*	*d*(Å)**	I_{theo}***	Δθ(°)
	(100)	31.73	2.82	471.0	0.173	754	31.7771	2.813	564	0.0471
	(002)	34.42	2.60	423.9	0.194	1754	34.4329	2.601	414	0.0129
	(101)	36.22	2.20	413.4	0.200	2236	36.2641	2.475	999	0.0441
	(102)	47.51	1.91	409.2	0.210	549	47.5543	1.91	216	0.0443
ZnO	(110)	56.58	1.62	355.6	0.251	536	56.6118	1.624	312	0.0318
	(103)	62.83	1.47	334.4	0.275	776	62.8785	1.476	275	0.0464
	(200)	66.35	1.41	396.7	0.237	104	66.3964	1.406	41	0.0464
	(112)	67.96	1.38	386.7	0.245	440	67.9695	1.378	222	0.0095
	(201)	69.08	1.36	398.1	0.240	176	69.1081	1.358	109	0.0281

*2θ(°), is the theoretical value of the diffraction angle;
**d(Å) is the theoretical value of the lattice spacing, and
***I_{theo} is the theoretical value of the intensity.

Table 2. The diffraction angle (2θ), lattice spacing (*d*), intensity (*I*) and crystallite size (*D*) of ZnO:Fe thin films

	(*hkl*)	2θ(°)	*d*(Å)	*D*(Å)	β(°)	*I*(a.u.)	2θ(°)*	*d*(Å)**	I_{theo}***	Δθ(°)
	(100)	31.65	2.825	502.2	0.162	400	31.7771	2.813	564	0.1194
	(002)	34.33	2.605	498.5	0.160	2002	34.4329	2.601	414	0.0911
	(101)	36.16	2.482	250.5	0.330	2427	36.2641	2.475	999	0.0921
	(102)	47.38	1.917	490.5	0.170	833	47.5543	1.910	216	0.1576
ZnO:Fe	(110)	56.40	1.632	356.7	0.250	339	56.6118	1.624	312	0.2016
	(103)	62.69	1.481	414.2	0.220	1057	62.8785	1.476	275	0.1724
	(200)	66.21	1.410	521.3	0.180	62	66.3964	1.406	41	0.1682
	(112)	67.76	1.382	495.4	0.190	547	67.9695	1.378	222	0.2010
	(201)	68.88	1.362	500.0	0.190	229	69.1081	1.358	109	0.2182

* 2θ(°), is the theoretical value of the diffraction angle;
** d(Å) is the theoretical value of the lattice spacing, and
*** I_{theo} is the theoretical value of the intensity.

where $a_0 = 3.249$ Å and $c_0 = 5.202$ Å. From equation (2), we deduce the cell volume using equation (3):

$$\frac{1}{d^2} = \frac{4}{3}\left(\frac{h^2 + hk + k^2}{a^2}\right) + \frac{l^2}{c^2}, \quad (2)$$

$$V = \frac{\sqrt{3}}{2}a^2c = 0.866a^2c. \quad (3)$$

The lattice spacing (*d*), intensity (*I*) of a plane (*hkl*) and the angle of diffraction (2θ) at the phases identified along with (*hkl*) planes of the thin films are given in Tables 1 and 2 for the u-ZnO and ZnO:Fe, respectively.

The mixing of the dopant with the host matrix of ZnO is clearly indicated by the variation of the lattice constants and by the slight shift of the diffraction peaks. In addition, this slight displacement is related to a state of stress of materials. The residual stress (*s*) in the thin films plane can be calculated using the biaxial strain model along the c-axis direction according to equation below as in [12]:

$$s(\text{GPa}) = -233\frac{C - C_0}{C_0}, \quad (4)$$

where the constant 233 is equal to $[2C_{13}^2 - C_{33}(C_{11} + C_{12})]/2C_{13}$.

$C_{JCPDS} = C_0 = 5.202$ Å, $C_{11} = 209.7$ GPa, $C_{12} = 121.1$ GPa, $C_{13} = 105.1$ GPa, and$C_{33} = 210.9$ GPa are the elastic stiffness constants of the bulk zinc oxide. The lattice constant (*C*) is compressed, indicated by the negative values of the residual strain of the thin films (see Table 3). Consequently, the layers are under a compressive stress, due to the nature of the substrate.

The average grain size was calculated using the Debye Scherrer's equation [9] and is given in Table 3. We remark here that the crystallite size increases in the u-ZnO from 35 nm to 40 nm after iron incorporation

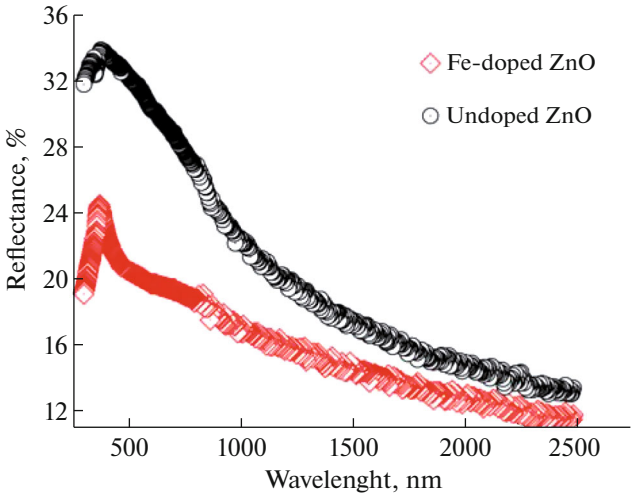

Fig. 4. Reflectance of u-ZnO and ZnO:Fe films.

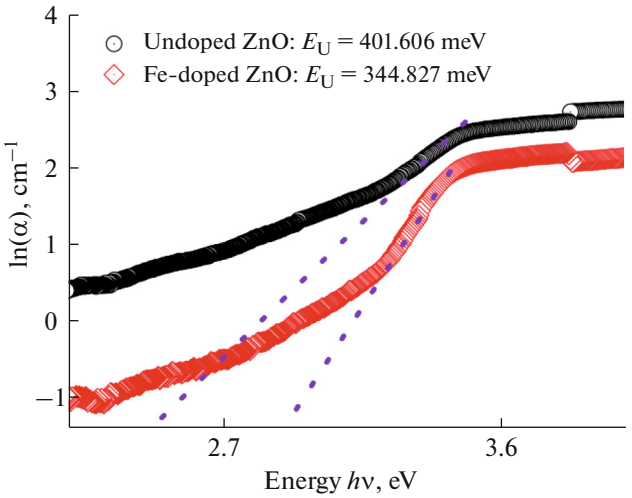

Fig. 6. Urbach plots (inset plots) of u-ZnO and ZnO:Fe films.

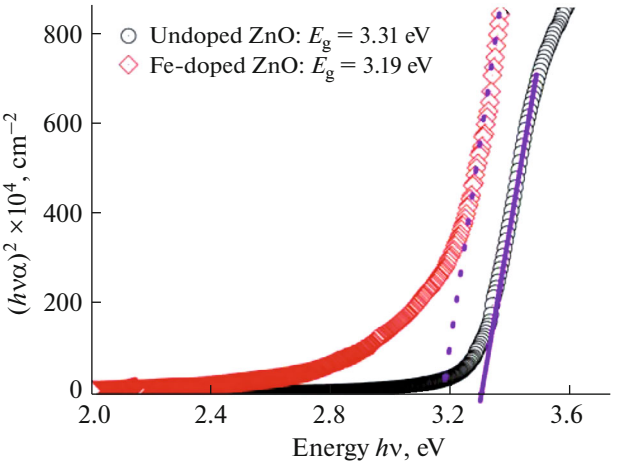

Fig. 5. Plots of $(\alpha h\nu)^2$ versus $(h\nu)$ of u-ZnO and ZnO:Fe films.

in the zinc oxide thin films. The crystallite size measurements agree well with the SEM observation.

Optical Characterization

The reflectance spectra of both u-ZnO and ZnO:Fe thin films are shown in Fig. 4.

The reflectance was less than 20% in the visible region. The absorption (α) of the thin films wasmeasured from the transmittance spectra, and the optical band gap E_g was deduced from the following equation:

$$\alpha = A\left(h\nu - E_g\right)^n, \quad (5)$$

where $h\nu$ is the photon energy, E_g is the band gap, A is the edge parameter and $n = 1/2$ in the case of ZnO which is one of the most important multifunctional *n*-type direct band gap semiconductors [13]. The optical band gaps E_g of both u-ZnO and ZnO:Fe films are illustrated in Fig. 5.

The band gap for the u-ZnO thin films was 3.31 eV and for the ZnO:Fe ones—3.19 eV. The change of the optical band gap of ZnO:Fe may be attributed to the band shrinkage effect because of increasing carrier concentration.

It is also assumed that the absorption coefficient near the band edge shows an exponential depen-dence on the photon energy as is given by equation (6) as in [9]:

$$\alpha = \alpha_0 \exp\left(E/E_U\right), \quad (6)$$

where E is the photon energy, α_0 is a constant and E_U is the Urbach energy which refers to the width of the exponential absorption edge. The Urbach energy is the width of the bands of localized states in the band gap. The Urbach energys E_U of both u-ZnO and ZnO:Fe films are illustrated in Fig. 6.

The E_U values were in the range of the previously reported values (0.1–0.6 eV) [14]. Our results showed

Table 3. Structural parameters of u-ZnO and ZnO:Fe thin films

	a, Å	*c*, Å	Volume, Å^3	Cristal size, nm	*c*/*a*	*S*, GPa
u-ZnO	3.262	5.206	47.92	35	15.941	–0.179162
ZnO:Fe	3.254	5.211	47.78	40	16.014	–0.403114
ZnO JCPDS card	3.249	5.202	47.59	–	16.023	–

a decrease in the Urbach energy due to the donor levels of zinc atoms interstitial. The optical parameters of the u-ZnO and ZnO:Fe thin films are summarised in Table 4.

Table 4. Optical parameters of u-ZnO and ZnO:Fe thin films

	Transmission, %	E_G, eV	E_U, meV
u-ZnO	88.5	3.31	401.606
ZnO:Fe	87.2	3.19	344.827

X-ray Photoelectron Spectroscopy Characterization

The element bonding of ZnO:Fe films was examined by the XPS and is-shown in Fig. 7. The high-resolution scanning information provided in Figs. 8a, 8b, 8c is for the separate analysis of three elements: oxygen, zinc, and iron, respectively.

The corresponding XPS results of the annealed ZnO:Fe thin film shows the high-resolution XPS spectra of Zn2*p*, O1*s*, and Fe2*p*. The binding energy of the $Zn2p_{3/2}$ remains to be 1020.48 ± 0.10 eV. This shows that Zn exists only in the oxidized state [9]. The O1s peak can be consistently fitted by three components centered at 529.48 ± 0.10 eV, 531.04 ± 0.10 eV, and 529.11 ± 0.10 eV, respectively. A low binding energy component centered at 529.48 ± 0.10 eV of the O1s spectra is attributed to O^{2-} ions on the quartzite structure of a hexagonal Zn^{2+} ion array, surrounded by Zn atoms with their full complement of nearest-neighbor O^{2-} ions [15]. A high binding energy component located at 531.04 ± 0.10 eV is probably attributed to the presence of loosely bound oxygen on the surface of ZnO:Fe thin films and a low binding energy 529.11 ± 0.10 eV is attributed to the diatomic anion OH^- [9].

Figure 7 shows that the binding energy values of Fe2*p* are 710.47 ± 0.10 and 723.62 ± 0.10 eV. The component centered at 723.62 eV based on the Gaussian fitting achieved with 5 at % iron concentration and heat treatment at 580°C in the ambient air, was a characteristic of Fe^{3+} [16]. This characte-ristic confirmed that Fe^{3+} ions were introduced into the ZnO crystal lattice because the Fe ions (0.55 Å) have shorter ionic radii than Zn ions (0.74 Å). The major Fe ions in ZnO:Fe polycrystalline are confirmed by the XPS studies. No metallic iron peak centered at 72.7 ± 0.06 eV appeared in the XPS results. This is in good agreement with the resultant of no Fe_2O_3 or other second phase obtained. The Fe content is estimated to be about 6.5 atomic percent (at %) from the analysis of the XPS spectra. Furthermore, to determine the concentration in these samples, the EDS analysis was performed and traced in detail.

Energy-Dispersive Spectroscopy Characterization

In order to determine the elements of the prepared samples of u-ZnO and ZnO:Fe thin films, the EDS analyses were performed and the results are shown in Fig. 9.

The EDS spectra indicate that the films as-prepared mainly contain three elements: Zn, O, and Fe. This is good agreement with the results of the XPS spectra. Apart from that, the Cu and C peaks in the EDS originate from the TEM micromesh grid. The Al, Si, K and Ca elements presented in Table 5b originated from the nature of the glass substrate used.

The characteristic peaks of O appeared at 0.5 keV in u-ZnO and at 0.54 keV in ZnO:Fe while the characteristic peaks of Zn appeared at 1.06 keV in u-ZnO and at 1.1 keV in ZnO:Fe [17]. The results clearly showed that the films were mainly composed of zinc and oxygen, the atomic ratio ([O]/[Zn]) was 1.17 for undoped layers and 1.47 for doped ones. In addition, these high ratios indicated that the films were rich in oxygen. The Fe peaks were observed in ZnO:Fe polycrystalline at 1.25 and 6.38 keV, which indicates that a ZnO:Fe semiconductor was successfully synthesized by the sol-gel method and Fe^{3+} ions occupied the place of the Zn^{2+} ions in the sample, as is confirmed by the XPS studies, XRD data, and UV-spectra. The solutions'

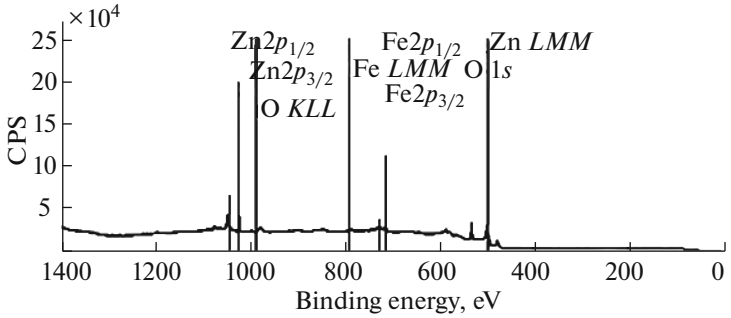

Fig. 7. XPS survey spectrum of ZnO:Fe thin films.

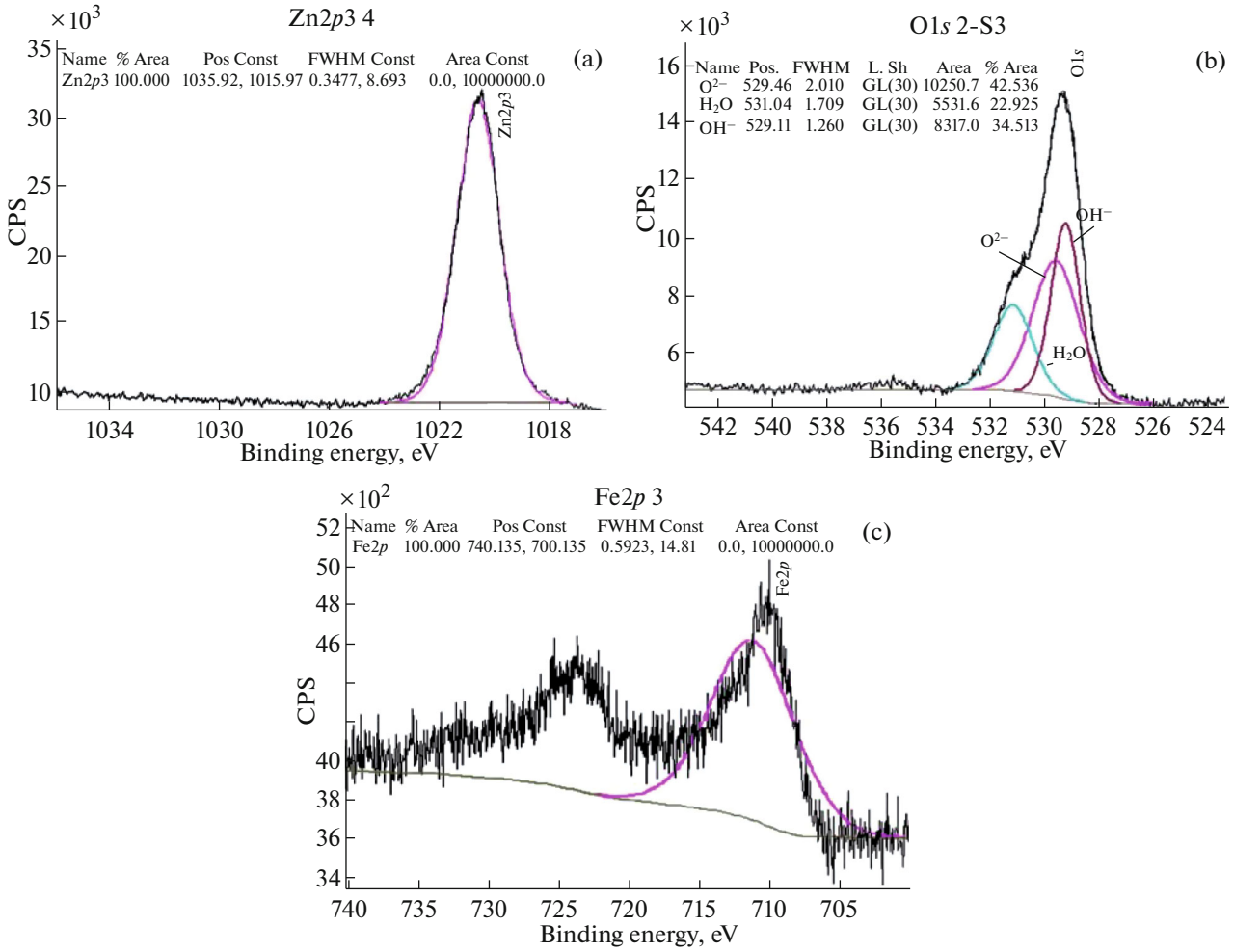

Fig. 8. XPS spectrum data of narrow scan: Zn2*p*3/2 (a), O1*s* (b), and Fe2*p*3/2 (c) of ZnO:Fe films.

dosage and the doping of the films have been demonstrated by the EDS studies and the values of the EDS analysis are resumed in Tables 5a, 5b.

To sum up, the EDS results indicated that thin films of a high quality of both u-ZnO and ZnO:Fe were obtained.

Table 5a. The EDS analysis of u-ZnO and ZnO:Fe pure ZnO thin films

Element	AN	Series	[wt %]	N, wt % *	N, at % *	Error wt % *
Oxygen	8	K-series	19.87151	19.87151	50.12324	0.475557
Silicon	14	K-series	2.973969	2.973969	4.273327	0.106216
Zinc	30	K-series	69.89081	69.89081	43.13408	1.456861
Tin	50	L-series	7.263704	7.263704	2.46935	0.206076
Sum			100	100	100	

Table 5b. The EDS analysis of ZnO:Fe thin films

	O	Al	Si	Cl	K	Ca	Fe	Zn
Position 1	53.666	0	1.133	2.240	1.050	0.244	5.296	36.372
Position 2	51.123	0.041	1.659	1.047	0.737	0.420	3.096	41.883
Position 3	52.049	0.733	3.039	4.532	2.156	0.464	5.694	31.332
Position 4	40.787	0.905	3.668	3.675	1.416	0.652	5.438	43.459
Mean value	49.406	0.420	2.374	2.873	1.340	0.445	4.880	38.262
Sigma	5.8417	0.4669	1.1789	1.5414	0.6106	0.1677	1.2036	5.5292
Sigma mean	2.9208	0.2334	0.5895	0.7707	0.3053	0.0838	0.6018	2.7646

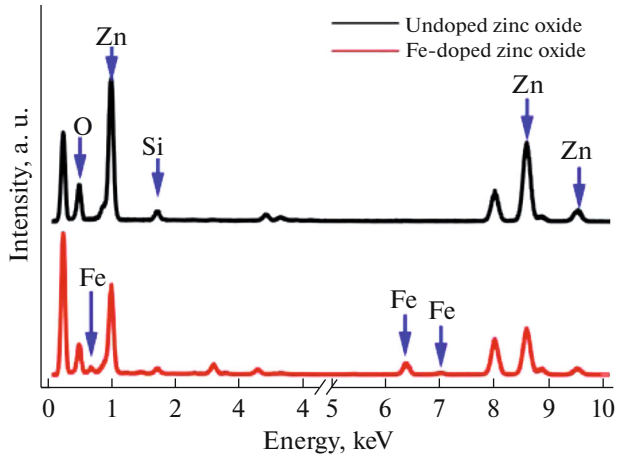

Fig. 9. EDS spectra of u-ZnO and ZnO:Fe thin films.

CONCLUSIONS

Both u-ZnO and ZnO:Fe thin films have been prepared by a sol-gel process using the technique of coating. The doping has displayed its important role in changing the structure and improving the crystallinity of polycrystalline ZnO whose the layers of the as-grown films were under a compressive stress, as was supported by the SEM and XRD analyses. The mixing of the dopant with the host matrix of ZnO was clearly illustrated in the optical transmittance measurement (UV-VIS) via decreasing the optical band gap and expanding the Urbach tail, which was confirmed by the XPS studies. The solutions dosage and the doping of the films have been demonstrated by the EDS studies that indicated a high quality of both u-ZnO and ZnO:Fe thin films.

ACKNOWLEDGMENTS

This work was supported by all members of the Laboratory of Electron Microscopy and Materials-Sciences at the University of Science and Technology of Oran, Algeria and by the Team NanoForm from the Laboratory ICB at the University of Burgundy, Dijon, France.

REFERENCES

1. Gyu-Chul, Y., Chunrui, W., and Won, I.P.A., *Semicond. Sci. Technol.*, 2005, vol. 20, no. 4, p. 22. doi 10.1088/0268-1242/20/4/003
2. Baoquan, S. and Henning, S., *Nano Lett.*, 2005, vol. 5, no. 12, pp. 2408–2413. doi 10.1021/nl051586w
3. Djurisic, A.B., Ng, A.M.C., and Chen, X.Y., *Prog. Quantum Electron.*, 2010, vol. 34, no. 4, pp. 191–259.
4. Chitra, A., Oliver, K., Gunnar, S., Hilde, S., et al., *Thin Solid Films*, 2003, vol. 442, no. 2, pp. 167–172.
5. Buchholz, D.B., Liu, J., Tobin, J.M., Zhang, M., et al., *ACS Appl. Mater. Interfaces*, 2009, vol. 10, no. 1, pp. 2147–2153. doi 10.1021/am900321f
6. Inamdar, D.Y., Arjun, K., Dubenko, P.I., Naushad, A., et al., *J. Phys. Chem. C*, 2011, vol. 115, no. 48, pp. 23671–23676. doi 10.1021/jp205854p
7. Baranowska-Korczyc, A., Reszka, A., Sobczak, K., Sikora, B., et al., *J. Sol-Gel Sci. Technol.*, 2012, vol. 61, pp. 494–500. doi 10.1007/s10971-011-2650-1
8. Xiaohong, S., Xudong, H., Yongchao, W., Rui, X., et al., *J. Phys. Chem. C*, 2015, vol. 119, no. 6, pp. 3228–3237. doi 10.1021/jp5124585
9. Zegadi, C., Abdelkebir, Kh., Chaumont, D., Adnane, M., et al., *Adv. Mater. Phys. Chem.*, 2014, vol. 4, no. 5, pp. 93–104. doi 10.4236/ampc.2014.455012
10. Chelouche, A., Djouadi, D., and Aksas, A., *Eur. Phys. J. Appl. Phys.*, 2013, vol. 64, p. 10304. doi 10.1051/epjap/2013130336
11. Kaneva, N.V. and Dushkin, C.D., *Bulg. Chem. Comm.*, 2011, vol. 43, no. 2, pp. 259–263.
12. Liu, C., Meng, D., Pang, H., Wu, X., et al., *J. Magn. Magn. Mater.*, 2012, vol. 324, no. 20, pp. 3356–3360. doi 10.1016/j.jmmm.2012.05.054
13. Wanga, J., Elamurugua, E., Sallet, V., Jomard, F., et al., *Appl. Surf. Sci.*, 2008, vol. 254, pp. 7178–7182. doi 10.1016/j.apsusc.2008.05.321
14. Campbell, D.J., Higgins, D.A., and Corn, R.M., *J. Phys. Chem.*, 1990, vol. 94, pp. 3681–3689. doi 10.1021/ j100372a060
15. Clakes-Olsson, O.A. and Hornstrom, S.E., *Corros. Sci.*, 1994, vol. 36, pp. 141–151. doi 10.1016/0010-938X(94)90115-5
16. Mustin, C., De Donato, P., Benoit, R., and Erre, R., *Appl. Surf. Sci.*, 1993, vol. 68, pp. 147–158.
17. Xiaojuan, W., Zhejiang, W., Lingling, Z., Xuan, W., et al., *J. Nanomater.*, 2014, vol. 2014, pp. 792102–792108. doi 10.1155/2014/792102